# FLEET Velocimetry in the Common Research Model's Wing Wake

Daniel T. Reese[1], Paul M. Danehy[2], Eric L. Walker[3], and S. Melissa Rivers[4]
*NASA Langley Research Center, Hampton, VA, 23681, United States*

William K. Goad[5]
*Jacobs Technology, Inc., Hampton, VA, 23666, United States*

**Femtosecond laser electronic excitation tagging was used to make velocity measurements in the wake of the wing of the Common Research Model (CRM). Experiments were performed in the NASA Langley Research Center's National Transonic Facility over a range of tunnel operating conditions. Pressures ranged from 205 to 411 kPa, temperatures from 278 to 323 K, and Mach from 0.1 to 0.9. Velocity was also determined over a range of model angles of attack. Time-averaged velocity results were obtained in both air and nitrogen, while single-shot velocity was obtained under certain tunnel operating conditions. Spatially-resolved, two dimensional, single component velocity measurements were achieved using a newly-developed laser scanning technique, which proved sufficiently sensitive to measure an approximately 5% velocity deficit in the wing wake region of the CRM.**

## I. Introduction

Femtosecond laser electronic excitation tagging (FLEET) has seen increased use in recent years due to the technique's relatively simple setup and ability to provide unseeded measurements of velocity in air and nitrogen. FLEET works by focusing a femtosecond laser to dissociate/ionize molecular nitrogen [1], thereby "tagging" a region of fluid. This tagged gas then advects downstream with the flow of interest, and photons emitted during the long-lived (10s of μs) recombination can be captured on a camera so the fluid can be tracked through sequential imaging. The technique has been used to make velocity measurements in a jet [2], around a transonic airfoil [3], and in the freestream of subsonic, transonic, and hypersonic flows [4-6]. Most recently, FLEET was applied in the National Transonic Facility (NTF) to obtain freestream velocity measurements upstream of a survey rake [7].

In the present work, FLEET was applied to the wake region behind the wing of the Common Research Model (CRM) in the NTF. Velocity measurements were obtained at a variety of tunnel operating conditions by adjusting the pressure, temperature, and Mach number of the flow. The angle of the model with respect to the freestream was also varied throughout the test to provide velocity measurements at several angles of attack. Ref. [7] describes in detail the laser penetration system (LPS) used to direct the laser beam into the facility, through the high-density plenum and into the test section. Hardware has recently been added to the LPS to allow the FLEET signal to be scanned across the spanwise direction of the tunnel. This scanning method provided a spatially-resolved, two-dimensional velocity map in the wake region of the CRM wing, showing the presence of a well-defined velocity deficit region. The following section describes the experimental facility and the setup used to capture FLEET data. Section III outlines the data processing performed to obtain wake velocity measurements. Section IV presents and discusses the experimental results. Section V details future work, while Section VI provides conclusions.

[1] Research Engineer, AIAA Member.
[2] Senior Technologist for Advanced Measurement Systems, AIAA Associate Fellow.
[3] Chief Engineer for Test Operation Excellence, AIAA Associate Fellow.
[4] Aerospace Engineer, Configuration Aerodynamics Branch, Senior Member AIAA.
[5] Technical Specialist, ASCET.

## II. NTF Facility & Experimental Setup

NTF is a fan-driven, closed-circuit, cryogenic wind tunnel located at NASA Langley Research Center. This wind tunnel allows for the testing of scaled models at flight-accurate Reynolds numbers, which is ideal for studying the aerodynamic effects experienced (and caused) by the vehicle in flight. The NTF has a double-walled construction, where an outer shell contains the high pressure, and an inner test section serves as the channel through which the test gas flows. In nitrogen mode the tunnel is capable of reaching temperatures as low as 116 K, and in air mode temperatures can reach 322 K. Total pressure in the tunnel can reach 860 kPa, while Mach numbers experienced during testing range from approximately 0.1 to 1.2. The test section of the wind tunnel is 7.62 m long, with a cross section of 2.5 m by 2.5 m. The NTF is equipped with a data acquisition system (DAS) that allows for the acquiring, processing, recording, and displaying of test data.

While optical access is limited in NTF, recent modifications to the facility have provided a method of transmitting a laser beam from outside of the tunnel into the test section [7]. Using the laser penetration system (LPS) first described in Ref. [7], the final optical assembly at the end of the LPS was modified to simultaneously increase the FLEET signal (relative to that obtained in the previous test) while affording the ability to scan the location of the FLEET velocity measurement within the test section. This was accomplished by replacing a wedge prism (which caused a factor of two loss in signal) with a pair of mirrors, the final of which was remotely-adjustable. Using this setup, the FLEET signal could be directed within the field of view of the camera, which was housed in a pressure vessel maintained at roughly one atmosphere and room temperature. Several other components were also located within the camera enclosure; most notably a high-speed intensifier used to provide multiple exposures of the FLEET signal on a single imaging frame, as well as a remotely-adjustable focus ring used to re-focus the intensifier on the FLEET signal as it was scanned towards or away from the camera. Further details of the camera enclosure can be found in [7].

The Common Research Model (CRM) was installed inside the test section for the current set of experiments. The CRM wind tunnel model is a sting-mounted 2.7% scale model of a contemporary supercritical transonic wing and fuselage that is representative of a widebody commercial transport aircraft. The CRM was designed for a cruise Mach number of 0.85 and a corresponding design lift coefficient of 0.5 [8]. The aspect ratio is 9.0, the leading edge sweep angle is 35°, the wing reference area is 2796 $cm^2$, the wing span is 158.6 cm, and the mean aerodynamic chord is 18.9 cm. The geometry used during testing was the WBT0 (wing/body/tail=0°) configuration. The location of the FLEET interrogation region was downstream of the wing of the CRM, with the nominal-zero position approximately 13.5 cm spanwise away from the leading edge of the horizontal stabilizer.

## III. Data Processing

Raw data obtained during testing underwent a multi-step processing routine to provide the results presented and discussed in Section IV. Each step of data processing is described in detail within this section. Subsection A covers the dewarping and calibration of data. Subsection B outlines the detection of the peak FLEET intensity and the corresponding location of the signal. Subsection C discusses the determination of velocity from the signal location information.

### A. Dewarping and Calibration

Prior to testing, a target consisting of black dots in a regular grid pattern (a so called “dotcard”) was imaged at several locations along the tunnel spanwise direction inside of the test section for use in calibration. This target was used to provide the magnification and lens focus values at each scanning position for which data were obtained. By fitting the values for focus and magnification at the calibration points, the requisite settings at any point along the field of view can be determined. The target was also used to correct images for perspective and lens distortions by determining the dot locations using a custom centroid-finding algorithm, and then mapping each point to the expected location given the known target pattern. After determining the transformation in this way, the same transformation can be applied to FLEET data to correct for perspective and lens distortions. Because the distance between dots is known, this calibration also allows for the extraction of a scale factor used to bring pixels into physical units.

A typical time-averaged and dewarped FLEET signal is shown in Fig. 1(a), where the dark lines indicate the FLEET signal exposed at several time delays. In this image, the laser enters at a ~8° angle from the top of the image, and after approximately 10 ns, the first (left-most, darkest) FLEET signal is obtained. Subsequent exposures of the FLEET signal are taken every 10 μs, as the FLEET signal decays and advects rightward with the flow. A typical frame contains a total of five exposures.

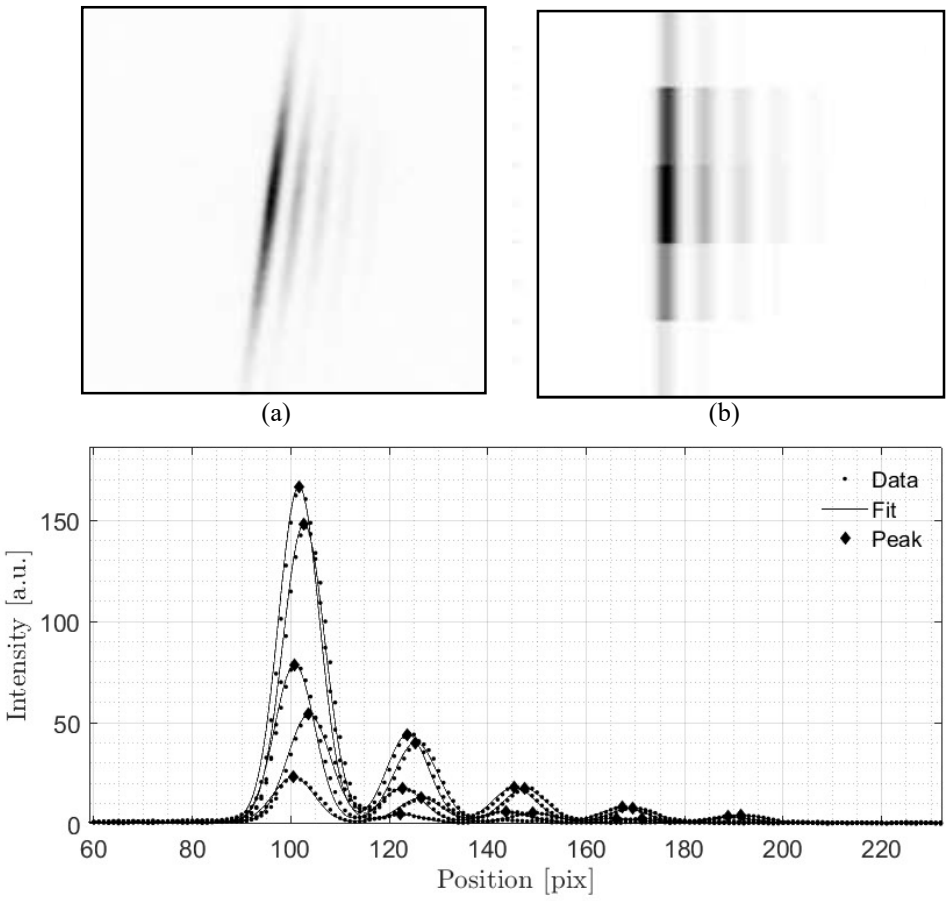


**Fig. 1 FLEET signal dewarping, rotation, binning, and peak finding.** (a) Time-averaged and dewarped FLEET signal in air. (b) Rotated and binned FLEET signal. (c) FLEET signal profiles for each bin of the rotated and binned FLEET signal image. Black diamonds indicate the detected peak signal intensity and location.

### B. Peak Signal and Location Detection

The first step in detecting the peak signal and location is to rotate the dewarped FLEET image to align the FLEET line with the vertical. Next, the image is binned into five rows in order to increase the signal-to-noise ratio (SNR) while maintaining spatial resolution. A rotated and binned STARFLEET image is shown in Fig. 1(b). For each bin, a FLEET signal profile is obtained, and is modeled as a series of Gaussians:

$$I = \alpha + \sum_{k=1}^{n} \beta_k e^{\frac{-(x-\gamma_k)^2}{\delta_k}}, \tag{1}$$

where $\alpha$, $\beta$, $\gamma$, and $\delta$ are fit parameters, and $n$ is determined by the number of exposures containing FLEET signal on the frame of interest. This model is shown fit to each of the five bins of data in Fig. 1(c) as black lines. Peak locations are then determined to sub-pixel accuracy by finding the locations of peak intensity in the fit model, which are shown in Fig. 1(c) as black diamonds. In this way, multiple peak intensities with corresponding locations can be determined for each bin, ultimately allowing for the extraction of velocity as a function of height along the image as described in the following subsection.

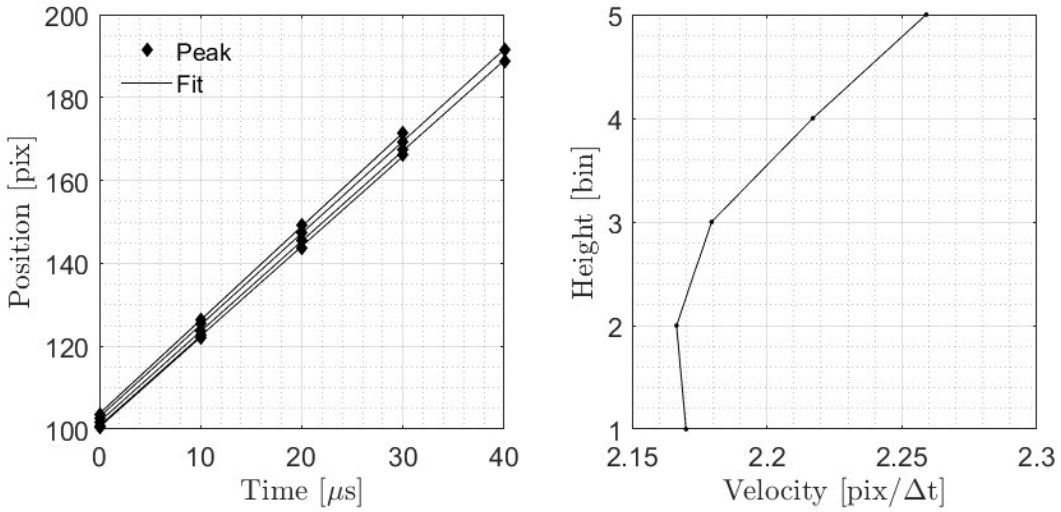


**Fig. 2 Velocity profile determination.** (a) Peak FLEET signal location as a function of time. Lines indicate the linear fit to data used to determine velocity. (b) Velocity profile as determined from the five line slopes in (a).

### C. Velocity Determination

With the locations of the peak FLEET signal detected with sub-pixel accuracy as described in the previous subsection, those locations can then be plotted against time, shown as black diamonds in Fig. 2(a). In this figure, four to five peaks were detected for each of the five bins of FLEET data, and a linear fit to these peak locations in time was used to determine the velocity for each bin, shown as lines in Fig. 2(a). Lines with a steeper slope indicate a larger velocity for the corresponding bin. The velocity (in pixels/$\Delta$t) as determined from the line slope is shown plotted for each bin in Fig. 2(b), where the points represent the velocity determined from the fit slope, and the line indicates the velocity profile calculated from the rotated and binned FLEET image. This velocity profile provides spatial information along the height of the FLEET signal for a single scan location, and corresponds to a single column of data in Fig. 3(a). By repeating this process for all eight scan positions, column-by-column, a two-dimensional velocity map can be assembled showing the velocity as a function of height and spanwise distance from the model, as shown in Fig. 3(a).

Because the FLEET signal cannot currently be scanned in the vertical direction, the model was rolled ±3° in order to extend the vertical domain of this velocity map. With the wing physically lower than the previous measurement (while maintaining the same angle of attack), the FLEET signal will probe velocities in a region above the initial measurement (relative to the wing), and another five-by-eight map can be added above the original one. Similarly, by rolling the model such that the wing is higher than used in the initial measurement, the FLEET signal will probe velocities in a region below the previous measurements, and a third five-by-eight map can be added below the other two. In this way, a fifteen-by-eight map can be built up from the three individual five-bin, eight-position maps obtained at each of the roll configurations. This larger velocity map is shown in Fig. 3(b). While large-scale features are visible in this velocity map, one important aspect of the two-dimensional map shown in Fig. 3(b) is that the units are in pixels/$\Delta$t; consequently, velocities (in pixels/$\Delta$t) steadily increase from left-to-right. The apparent increase in velocity is due to the imaging configuration, where the camera images from the right and has a diverging field of view, so the magnification of the pixels changes as the FLEET signal is scanned toward the camera along the spanwise direction. Using the calibration dot cards (as discussed in Section III.A) this map can be converted from spatial units of pixels and velocity units of pixels/$\Delta$t, into spatial units of mm and velocity units of m/s. The calibrated velocity map is shown in Fig. 3(c), where the velocity deficit of the wake region is clearly visible as a blue streak running horizontally across the map.

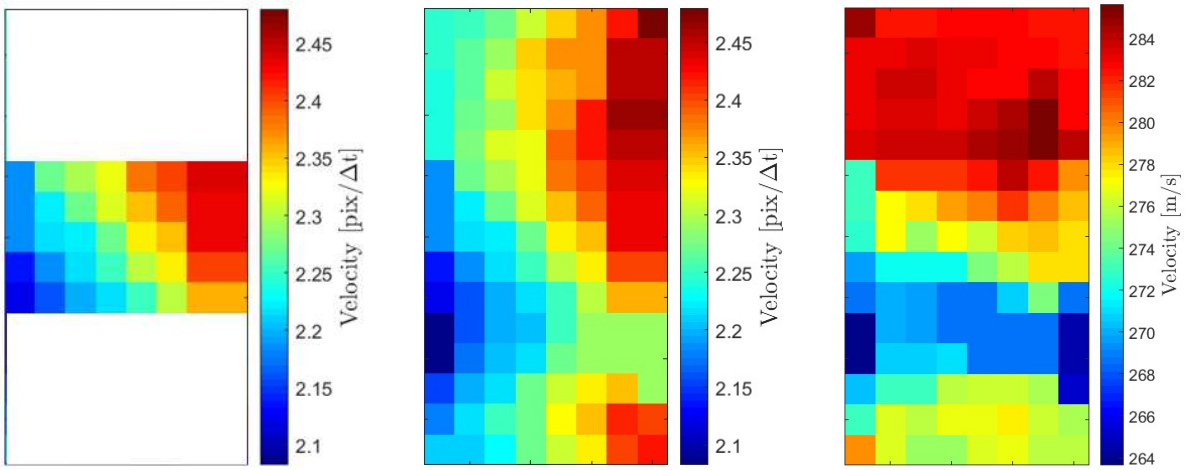


(a) (b) (c)

**Fig. 3 Two-dimensional velocity measurements using binned signal.** (a) Two-dimensional velocity sub-map for the zero-degree roll case. (b) Two-dimensional velocity map showing the spatial dependence of velocity in the region probed using FLEET. (c) Calibrated two-dimensional velocity map corrected to account for magnification effects. The horizontal axis in all three figures is pixel location (equally spaced, ½", or 12.7 mm, increments), and the vertical axis is based on the bins used for the velocity profiles. Data shown were taken in air at Mach 0.85, at a pressure of 210 kPa and a temperature of 322 K.

## IV. Experimental Results and Discussion

With an understanding of how the two-dimensional velocity maps described in the previous section were calculated, a more detailed look into the experimental results is explored in this section. Subsection A covers the two-dimensional velocity map results obtained using the laser-scanning technique, and subsection B outlines the dependence of FLEET results on the CRM angle-of-attack.

### A. Two-dimensional Velocity Maps

In addition to the simplified, low-resolution images shown in Fig. 3, the data obtained in this test can be reprocessed to obtain higher spatial resolution and more accurate velocity results. By taking a 20-row running average (rather than five bins of 20 pixels each) to increase SNR, improved resolution along the height of the velocity map can be attained. This higher-resolution velocity map can be seen in Fig. 4(a), and can be compared directly with the low-resolution velocity map shown in Fig. 3(c). The next step in improving velocity results involves accounting for a vertical shift in the FLEET signal. As the laser was scanned away from the model (toward the imaging camera), the FLEET signal was observed to move upwards in the corresponding images. By accounting for this vertical shift, as well as the spreading field of view of the camera, it is clear that there is overlap between the three five-by-eight sub-maps obtained by rolling the model. The vertical shift and overlap between velocity sub-maps can be clearly seen in Fig 4(b) where, by moving upward from the bottom of a column, velocity first decreases as the wake region is approached, then increases again as the wake region is exited. However, as the sub-map corresponding to zero roll is approached, the wake region is entered once again. Incorporating the overlap between the three five-by-eight pixel sub-maps shows the true structure of the wake region and allows the usage of physical spatial units, rather than pixels. A velocity map accounting for overlap between the three sub-maps is shown in Fig. 4(c). Finally, to compensate for the coarse spacing between scan positions and allow for better comparison with CFD, the velocity map shown in Fig. 4(c) can be interpolated and smoothed to provide a finer-resolution map, as shown in Fig. 4(d). The interpolated and smoothed velocity map is shown in relation to the CRM in Fig. 4(e).

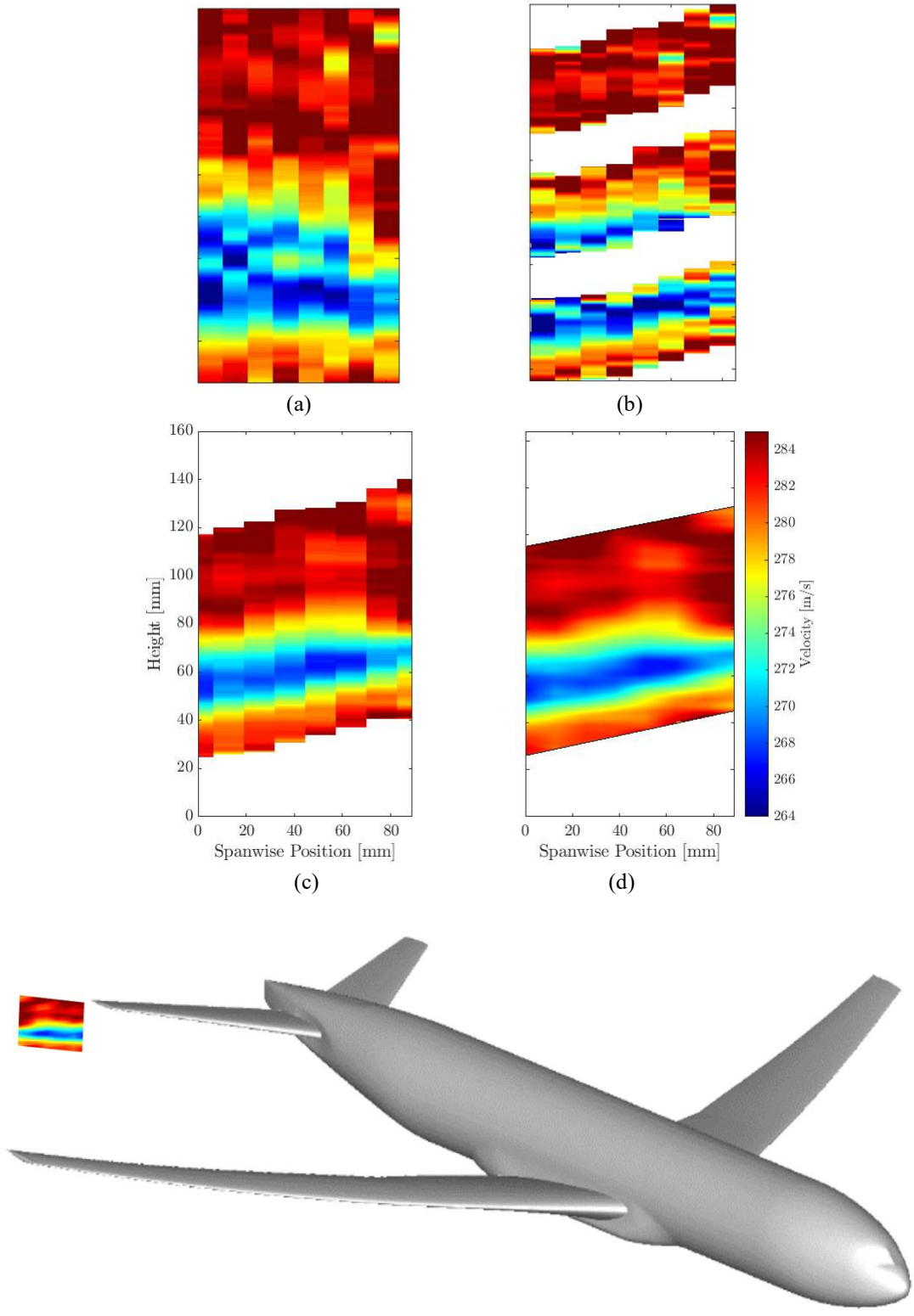


**Fig. 4 Results of the FLEET signal scan.** (a) Two-dimensional velocity map determined using a 20-row running average. (b) Velocity map accounting for vertical shift in FLEET signal that occurs during scanning. (c) Velocity map incorporating overlap between sub-maps. (d) Interpolated and smoothed velocity map. (e) Velocity map shown in relation to the CRM.

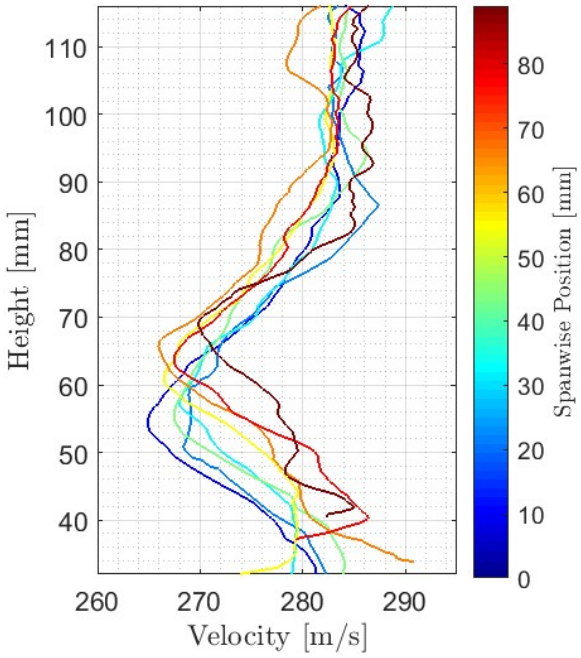


**Fig. 5 Velocity deficit profiles.** Profiles showing the velocity deficit in the CRM wing wake region at each spanwise position considered in this study.

By viewing profiles of the non-interpolated/smooth velocity map shown in Fig. 4(c), the spatial dependence of the velocity deficit in the CRM wing wake region is clearly visible. These velocity deficit profiles are shown in Fig. 5, where near-freestream velocity occurs from the top of the profile until near 90 mm, at which point the velocity drops to approximately 268 m/s, indicating that these measurements can resolve a ~5% velocity deficit. Additionally, the location of minimum velocity increases while the width of the wake region decreases as distance from the model body (spanwise position) is increased.

### B. Angle-of-attack Dependence

In addition to the laser scan that provided the velocity maps and spatially-varying deficit profiles shown in the previous subsection, a study on the effect of the CRM angle-of-attack (AOA) on the wake velocity profile was also carried out. By positioning the FLEET line at a single location and varying the AOA of the CRM, velocity profiles were obtained showing the effect of the model's attitude. Velocity profiles in the wing wake region for AOAs ranging from -2 to 9 degrees are plotted in Fig. 6, and show variations in profile structure as a function of angle-of-attack. At the lowest angle of attack (-2°) a strong velocity deficit is clearly present in the center of the profile, near a height of ~10 mm. This deficit region is shown to broaden and increase in height with increasing AOA, along with an overall increase in velocity. This trend continues until AOA=2-5°, when nominally-straight, near-freestream velocity profiles develop.

Beyond an AOA of 5 degrees, profiles show an overall reduction in velocity with increasing AOA. At these larger AOAs, profiles also show a dual-peak structure, where the peaks appear to converge with increasing AOA. The profile corresponding to AOA=6° shows peaks at approximate heights of 13 mm and 2 mm; by AOA=8°, the upper peak is shown to move downward to a height of ~11 mm, and the two peaks appear to merge near 8 mm by the largest AOA. Though these general trends are apparent for this particular flow condition, further investigation into this phenomenon is warranted before conclusive claims regarding flow physics of the CRM wake can be drawn.

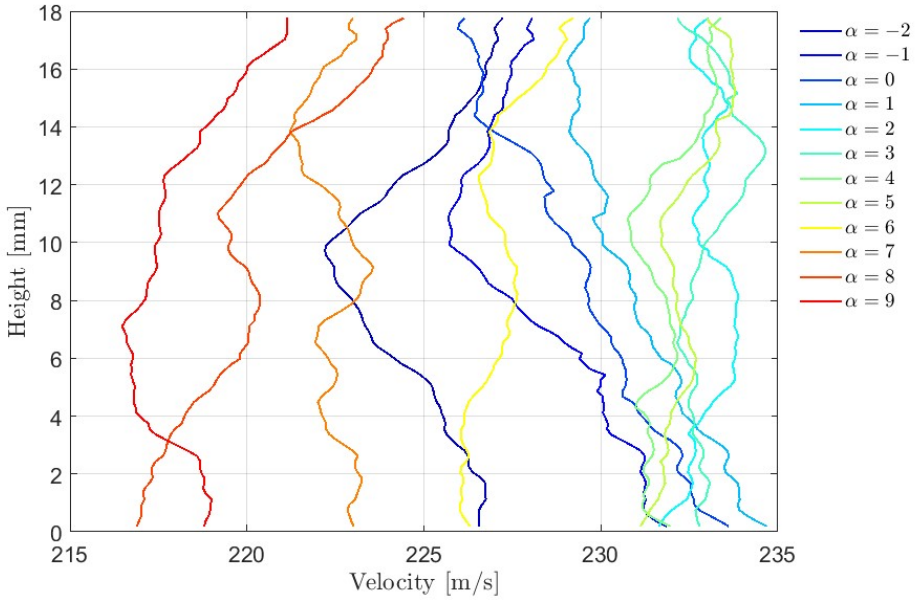


**Fig. 6 Velocity profiles at various angles of attack.** Profiles showing the velocity deficit in the CRM wing wake region at angles of attack ranging from -2 to 9 degrees. Data shown were taken in air at Mach 0.7, at a pressure of 233 kPa and a temperature of 322 K.

## V. Future Work

Though the binned data shown in Fig. 3 are low resolution (and the higher-resolution data shown in Fig. 4 have been spatially and temporally averaged), there are several ways to increase the resolution in future experiments. Primarily, it should be noted that the data shown in Fig. 3 were obtained while the tunnel was running at a pressure of 210.3 kPa, a temperature of 322 K, and with air as a test gas. Because the FLEET technique works best in high-density nitrogen [4], the signal-to-noise ratio (SNR) will greatly improve by increasing the pressure, decreasing the temperature, and switching to nitrogen as the test gas. Continual improvements to the LPS will also ultimately provide higher quality data, and will allow for measurements to be made at more extreme tunnel operating conditions. These improvements, along with a more favorable environment to the FLEET technique (i.e. higher density nitrogen) will allow for the capture of FLEET images with higher SNR. With increased SNR, the rotated FLEET image will be able to be broken into more bins (or potentially not require any binning), and the resolution along the vertical direction can be greatly improved.

Additionally, by increasing the number of scan positions, resolution of the velocity map can also be improved in the spanwise direction. Although the current studies used 12.7 mm spacing between the FLEET imaging locations, if the same 88.9 mm region is probed using 6.35 mm spacing, for example, the effective spanwise resolution can be doubled. In this way, finer spacing between scan positions will correspond to greater resolution along the spanwise direction. Improved SNR will also allow for singe-shot velocity measurements, yielding time-resolved velocity for each scanning position. Single-shot, time-resolved velocity measurements would also allow for the calculation of a 2D standard deviation map to compliment the velocity map obtained in the current study.

Although the laser beam can currently be scanned in the spanwise and streamwise directions, the ability to scan the FLEET line along the vertical direction could be implemented, thus removing the need to roll the model in order to expand the location mapped using FLEET. Additionally, using the same setup as used in the current studies, by adjusting the timings and filters used to capture the FLEET signal, Rayleigh scattering can be captured simultaneously. This would allow for the simultaneous measurement of density and velocity. Finally, automating the data acquisition would allow measurements to be made in more spatial locations and at many more operating conditions during future wind tunnel tests.

## VI. Conclusion

A modification to the newly-installed laser penetration system in NTF has allowed for two dimensional FLEET velocimetry measurements in the wing wake of the CRM. Testing was conducted over a range of tunnel operating conditions by independently changing the pressure, temperature and Mach number of the flow. Velocity measurements were obtained over a range of CRM angles-of-attack, and allowed for comparison of velocity profile structure as a function of AOA. The modifications to the optical assembly attached to the end of the LPS not only helped to increase the FLEET SNR, but also provided a new scanning capability to the system. This scanning technique provided a two-dimensional, single-component velocity map of the wake region of the CRM, and is able to resolve a ~5% velocity deficit.

## Acknowledgments

The authors wish to thank the entire NTF staff for their help in making improvements and modifications to the laser penetration system and associated optics. This work was supported by NASA's Aerosciences Evaluation and Test Capabilities (AETC) Portfolio under the leadership of Ron Colantonio and James Bell, lead for Test Technology. Funding for this project was also obtained from the NASA Langley Research Directorate. Funding for development of the FLEET technique was initially supported by NASA Langley's Internal Research and Development / Center Innovation Fund (IRAD/CIF) program.

## References

[1] Michael, J. B., Edwards, M. R., Dogariu, A., and Miles, R. B., "Femtosecond Laser Electronic Excitation Tagging for Quantitative Velocity Imaging in Air," *Applied Optics*, Vol. 50, No. 26, 2011, pp. 5158–5162.

[2] Peters, C. J., Danehy, P. M., Bathel, B. F., Jiang, N., Calvert, N. D., Miles, R. B., "Precision of FLEET Velocimetry Using High-speed CMOS Camera Systems," 31st AIAA Aerodynamic Measurement Technology and Ground Testing Conference, 2015, Dallas, TX.
DOI: 10.2514/6.2015-2565

[3] Burns, R. A. and Danehy, P. M., "Unseeded Velocity Measurements Around a Transonic Airfoil Using Femtosecond-Laser Tagging," *AIAA Journal* Vol. 55, No. 12, December 2017.
DOI: 10.2514/6.2017-0026

[4] Burns, R. A., Peters, C. J., and Danehy, P. M., "Unseeded Velocimetry in Nitrogen for High-Pressure, Cryogenic Wind Tunnels, Part 1: Femtosecond-Laser Tagging," *Measurement Science and Technology*, Vol. 29, No. 11, 115302, 2018.
DOI:10.1088/1361-6501/aade1b

[5] Dogariu, L. E., Dogariu, A., Miles, R. B., Smith, M. S., and Marineau, E. C., "Non-intrusive Hypersonic Freestream and Turbulent Boundary-Layer Velocity Measurements in AEDC Tunnel 9 using FLEET," In 2018 AIAA Aerospace Sciences Meeting, Kissimmee, Florida, USA, 2018. AIAA 2018-1769.
DOI: 10.2514/6.2018-1769

[6] Zhang, Y., Richardson, D., Beresh, S., Casper, K., Soehnel, M., Henfling, J., and Spillers, R., "Hypersonic wake measurements behind a slender cone using FLEET velocimetry," AIAA Aerodynamic Measurement Technology and Ground Testing Conference, 2019, Dallas, TX.

[7] Reese, D. T., Burns, R. A., Danehy, P. M., Walker, E. L., and Goad, W. K., "Implementation of a pulsed-laser measurement system in the National Transonic Facility," AIAA Aerodynamic Measurement Technology and Ground Testing Conference, 2019, Dallas, TX.

[8] Vassberg, J., Dehaan, M., Rivers, M., and Wahls, R., "Development of a Common Research Model for Applied CFD Validation Studies", AIAA Paper 2008- 6919, 26th AIAA Applied Aerodynamics Conference, June 2008 DOI: 10.2514/6.2008-6919.